Thermal Transitions in Perfluorosulfonated Ionomer Thin-Films

Meron Tesfaye,*[,†,‡] Douglas I. Kushner,[‡] Bryan D. McCloskey,[†,‡] Adam Z. Weber,[‡] and Ahmet Kusoglu*[,‡]

[†]Chemical and Biomolecular Engineering, University of California—Berkeley, Berkeley, California 94720, United States

[‡]Energy Technologies Area, Lawrence Berkeley National Laboratory, Berkeley, California 94720, United States

ABSTRACT: Thin perfluorosulfonated ion-conducting polymers (PFSI ionomers) in energy-conversion devices have limitations in functionality attributed to confinement-driven and surface-dependent interactions. This study highlights the effects of confinement and interface-dependent interactions of PFSI thin-films by exploring thin-film thermal transition temperature (T_T). Change in T_T in polymers is an indicator for chain relaxation and mobility with implications on properties like gas transport. This work demonstrates an increase in T_T with decreasing PFSI film thickness in acid (H^+) form (from 70 to 130 °C for 400 to 10 nm, respectively). In metal cation (M^+) exchanged PFSI, T_T remained constant with thickness. Results point to an interplay between increased chain mobility at the free surface and hindered motion near the rigid substrate interface, which is amplified upon further confinement. This balance is additionally impacted by ionomer intermolecular forces, as strong electrostatic networks within the PFSI—M^+ matrix raises T_T above the mainly hydrogen-bonded PFSI—H^+ ionomer.

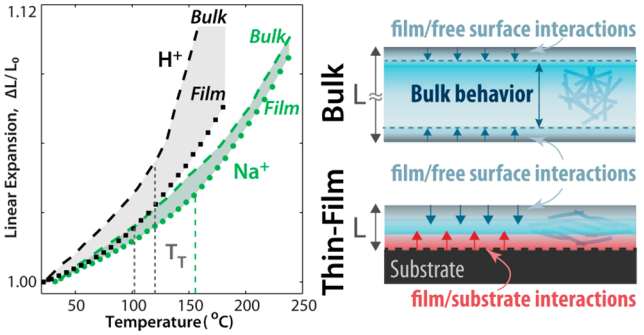

Polymer thin films are increasingly employed in coating applications, gas-separation systems, and energy-conversion devices, expanding the ubiquitous use of polymers, reducing cost, and material waste.[1−3] However, deviation of physical properties in thin polymer films (thickness < 100 nm) compared to bulk (thickness typically > 10 μm) adds significant uncertainty to their utility.[4−7] As the polymer film thickness approaches the molecular length scale, the influence of local surface and interface effects are amplified, resulting in a thin-film structure nonuniformity, stability differences, and variations in dynamics compared to bulk behavior.[3,8−10] Such is also the case for the ion-conducting polymer (ionomer) thin-films employed in polymer—electrolyte fuel cells (PEFCs) and related technologies. Perfluorosulfonated ionomer (PFSI) thin-films of 4—100 nm thickness are used as a solid-electrolyte binder in porous electrodes to improve catalytic activity (e.g., by creating pathways for proton transport to carbon-supported platinum in PEFC electrodes).[11,12] These thin-film ionomers behave dissimilarly from their corresponding bulk behavior, and are responsible for significant mass-transport resistances at the desired high current densities.[13−15] Studies focusing on nanoconfined ionomers have demonstrated the effect of thickness and substrate on morphology and domain orientation that alter an ionomer's proton conductivity on carbon and platinum surfaces.[16−19] Additionally, changes in ionomer ion-exchange capacity (inverse of the equivalent weight (EW)), variability in processing conditions, and differences in surface wettability and interaction have already been proven to impact mechanical properties and water-uptake capacity of ionomer thin-films.[19−25] Following these trends, it is reasonable to presuppose similar nanoconfinement effects on gas permeability to explain the aforementioned inferred ionomer thin-film gas-transport resistances.[26] However, a direct correlation of gas transport to confinement-driven parameters in ionomer thin-films has yet to be established.

Gas transport through dense polymers involves dissolution of gas at the membrane surface followed by a transport process, which is driven by a chemical potential gradient through the membrane and available free-volume in the polymer.[27] Accessible free-volume is a function of penetrant gas size and type as well as the chemical and physical nature of the polymer. In bulk PFSI, EW andside-chain length and chemistry can dictate polymeric packing, torsional movement, and relaxation of chains required for gas adsorption, solubility, and permeation.[27−30] In thin-film PFSI, this physicochemical phenomenon is exacerbated by presence of local interfaces and finite size effects that alter PFSI's structural relaxation behavior.[31,32] One broad physical descriptor correlating bulk and thin-film polymer chain mobility required for free-volume, gas dissolution, and permeability is the glass-transition temperature, T_g.[33] In a highly confined system, like that of an ionomer thin-film coating an electrocatalyst, T_g can serve as a characteristic thermodynamic transition of structural

relaxation correlating chain packing and mobility with gas transport.[3] Quantifying this transition temperature of nano-confined ionomers at and near surfaces is the focus of this study.

A major challenge in utilizing T_g as a single marker for PFSI relaxation behavior, as is frequently done in neutral homopolymers, is the presence of multiple thermal transitions (T_T) in bulk PFSI and their long-debated nature and source.[34−37] PFSIs are random copolymers composed of hydrophobic tetrafluoroethylene backbone units and perfluorovinyl ether side chains containing an ionic end group $-SO_3H$.[38,39] A consequence of this nanophase-separated, complex ionic structure is the presence of four thermal transitions (γ, β', β, α) that describe mechanical and relaxation behavior of PFSI. T_γ (−100 to −80 °C) occurs due to local short-range motion in the backbone $-CF_2-$ chains, independent of the counterion type (SO_3-M).[34,36] β' and β relaxation have been attributed to either the side-chain and main-chain motions in PFSI network, respectively.[36,40] T_β relaxation is considered equivalent to the T_g in classical glassy polymers, which marks the onset of transition from glassy (brittle) to rubbery (viscous) behavior.[37] For PFSI in H^+ form, β relaxations have been reported to be around −60 to 23 °C.[38] However, exchanging H^+ with different counterions (M^+) results in distinct dynamic-mechanical analysis peaks for the ether side-chain $T_{\beta'}$ (near −20 to −30 °C) and ionomer matrix, T_β (around 130−170 °C).[35,36] The final thermal transition, α-relaxation, T_α (87−120 °C in H^+ form and 210−240 °C in various M^+ form),[37,41,42] is attributed to relaxation of the clustered ionic domains scattered within the nonpolar ionomer matrix. Although the T_T are discussed here as distinct, local relaxations, small-scale chain motion are still likely to influence gas permeation by impacting segmental mobility, molecular packing, and free-volume independently and coupled with main-chain motion as exemplified in other polymers.[27,43] Taking this fact into account, this study aims to develop understanding of confinement-driven changes in T_T of PFSIs (Nafion and 3M) in the 30 to 250 °C range as a proxy for chain mobility and packing impacting critical properties like gas transport. Using substrate supported ionomer thin-films as model systems, the dependence of T_T on the electrostatic network and side-chain mobility is explored via metal counterion exchange (Na^+, Cs^+).

T_T in thin-film polymers can be obtained via volume expansion,[44] segmental mobility,[45] and viscoelasticity[46] tracking techniques. Figure 1 shows a normalized thickness profile of Nafion thin-films in acid (H^+) and cationic (Na^+ and Cs^+) forms obtained via in situ heated cell ellipsometry (see expanded details in SI). A change in the rate of thickness expansion at a specific temperature is defined as the PFSI T_T. Linear thermal-expansion coefficients (α_L) in pre- and post-transition temperature regimes are calculated via

$$\alpha_L = \frac{1}{L_o}\frac{\Delta L}{\Delta T} \quad (1)$$

where L_o is the ambient, dry thickness and ΔL and ΔT represent change in thickness and temperature, respectively. Figure 2 shows T_T and pre- and post-α_L of PFSI−H^+ as a function of thickness, extracted from similar measurements shown in Figure 1. The 1-dimensional thin-film expansion, α_L, is compared to the isotropic, 3-dimensional volumetric thermal-expansion coefficient, α_V, of bulk PFSI obtained

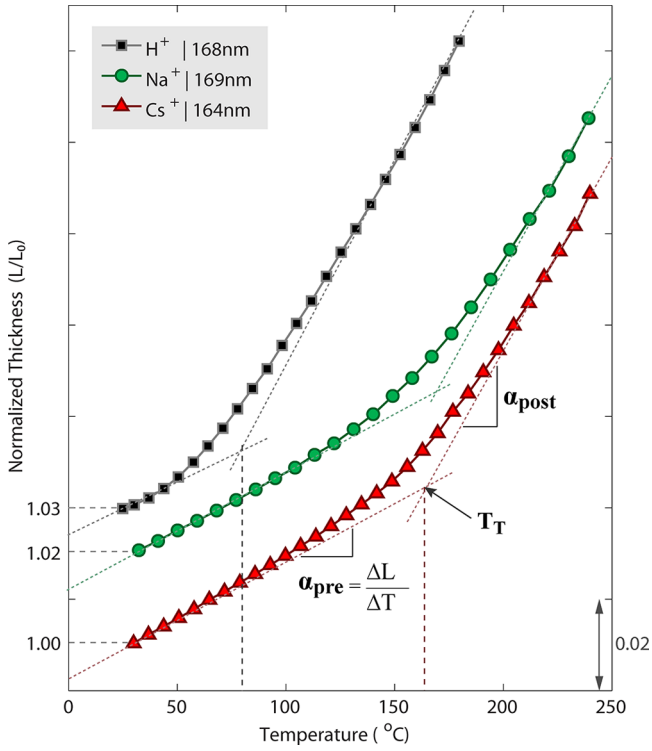

Figure 1. Change in normalized thickness (L/L_o) of Nafion thin-films with respect to dry thickness (L_o) during cooling used for calculating transition temperature (T_T) and pre- and post-transition expansion rate (α_{pre} and α_{post}). Curves are offset in the y-axis for improved visibility.

from average bulk linear expansion coefficient, where $\alpha_V \approx 3{\cdot}\alpha_{L,bulk}$ from refs 47 and 48. Both thin-film T_T and α_L demonstrate no significant correlation with PFSI EW (Figure 2). The relative difference between pre- and post-expansion rate and range of T_T observed for thin-film PFSI−H^+ indicates that T_T is likely T_α. The T_T of thin-film ionomers >100 nm in Figure 2a are lower than T_α of cast bulk Nafion in H^+ form (~87 °C),[38,49] and an increase in T_T with decreasing thickness is observed with some data variability. α_{pre} remains somewhat constant, while α_{post} decreases with decreasing thickness (Figure 2b), consistent with the raised T_T evaluated. Thermal transition and subsequent relaxation behavior in thin-film polymers is governed by chain conformation upon confinement, polymer dynamics at the free-surface/polymer and substrate/polymer interfacial interactions.[50] It is well documented that polymer chains adsorbed at attractive interfaces induce changes in orientation and local packing that results in a decreasing polymer density distribution away from the surface.[51,52] Spatially opposite to the polymer/substrate interface, the free-surface/polymer interface has unhindered mobility and enhanced configurational freedom, thereby improving long-range motions and lowering the T_T.[53−55] High wettability and low surface energy of the Si/SiO_2 support results in favorable adsorption of the PFSI−H^+ side-chain moieties,[19,56,57] pining ionomer chains, and increasing local packing near the ionomer/substrate interface in dry conditions. Consequently, PFSI−H^+ thin-films have significantly restricted chain mobility below the T_T, as is reflected by the low α_{pre}, as illustrated in the schematics in Figure 2. As the temperature exceeds T_T, entropically frozen ionomer chains gain enough thermal energy (kT) to break electrostatic interactions

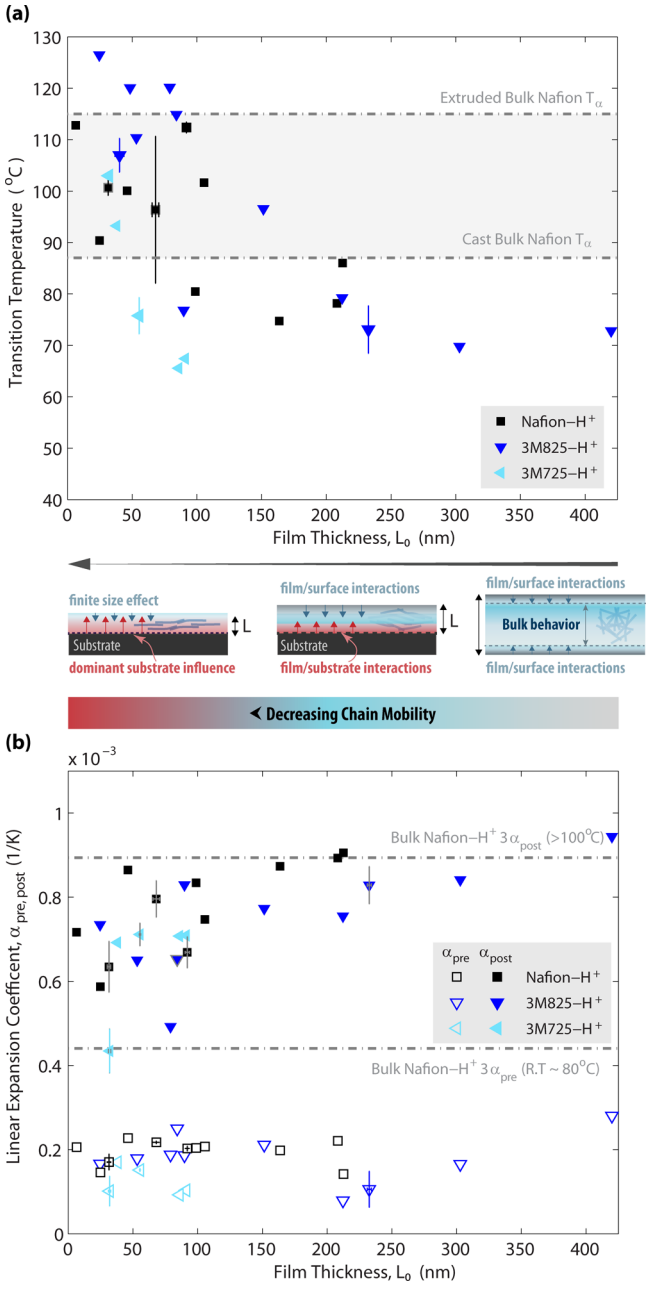

Figure 2. (a) Transition temperature and (b) linear expansion coefficient, α_{pre} and α_{post}, of thin-film PFSI–H^+ cast on Si/SiO_2 substrate compared to bulk Nafion linear expansion from ref 48.

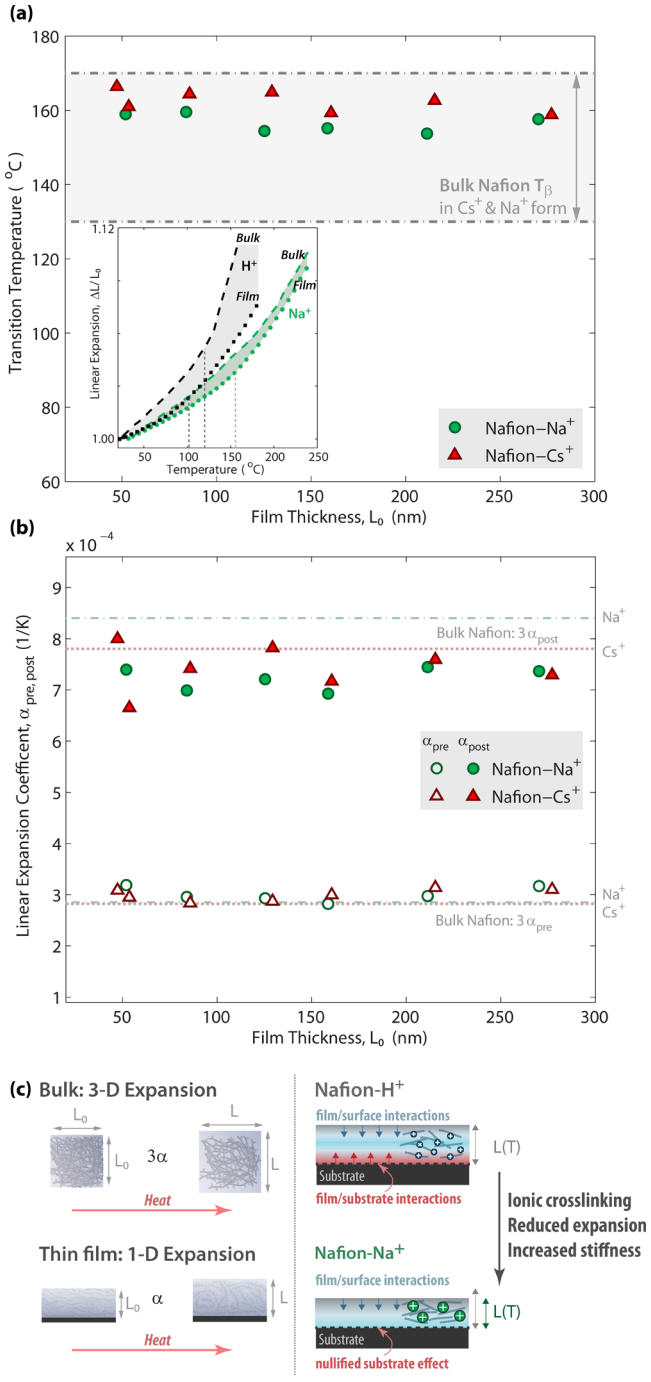

Figure 3. (a) Transition temperature and (inset) bulk vs thin-film linear expansion PFSI–H^+ vs PFSI–Na^+ form. (b) Linear expansion coefficient, α_{pre} and α_{post}, of thin-film PFSI–Na^+ and PFSI–Cs^+ cast on Si/SiO_2 substrate, compared to bulk Nafion linear expansion from ref 48. (c) Illustration of comparative volumetric expansion of PFSI in bulk vs thin-film and proton (H^+) vs cation (Na^+) form.

between PFSI–H^+ side chains and substrate, thereby relaxing the substrate-imposed constraints and resulting in an α_{post} similar to bulk PFSI. With a further decrease in thickness, the relative contribution of substrate interaction is amplified, resulting in a positive shift in T_T.

Figure 3 shows T_T, α_{pre}, and α_{post} of an ionomer thin-film in Na^+ and Cs^+ form as well as bulk film. Both α_{pre} and α_{post} are similar to the expansion rates observed in bulk Nafion around the β transition.[48] Here, unlike the PFSI–H^+ for which T_T was assigned to the α transition, the T_T for PFSI–M^+ is attributed to the β transition due to (1) only a single T_T observed for PFSI–M^+ thin-films and (2) the large positive shift (>100 °C) expected in both T_α and T_β with neutralization, as reported extensively in bulk PFSI literature.[34,37,40,58] PFSI–M^+ exhibits very small deviation from bulk T_β in the range of film thicknesses explored, contrary to PFSI–H^+ (Figure 3a). Table 1 compares PFSI T_α and T_β reported in literature with substrate-supported thin-film PFSI T_T measured in this study. Nature of counterion (H^+ vs M^+) can significantly alter relaxation behavior (α to β) causing a break in slope at high temperatures for strongly interacting, electrostatic network present in PFSI–M^+. Similar molecular origins have been shown for thermal and mechanical relaxation of bulk PFSI neutralized with various counterions.[37,58] Systematic spectro-

Table 1. Comparison of T_T for Bulk and Thin-Film PFSI in Different Forms

	T_β (°C)	T_α (°C)	refs
PFSI−H^+ (bulk)	−20 to −30	87−115	35−41
PFSI−M^+ (bulk)	130−170	210−240	
PFSI−H^+ (thin-film)			this work
>100 nm	T_T not observed	70−85	
<100 nm		70−130	
PFSI−M^+ (thin-film)			this work
>100 nm	160−170	T_T not observed	
<100 nm	160−170		

scopic and X-ray scattering studies are required to confirm the speculated nature of T_T measured in PFSI−H^+ and PFSI−M^+ as T_α and T_β, respectively.

At this point, it is critical to evaluate results discussed in Figures 2 and 3 as a complementary portrayal of segmental mobility dynamics in PFSI thin-films. High mobility near the free-surface/ionomer interface reduces T_T of PFSI−H^+ thin-films >100 nm relative to bulk, as represented schematically in Figure 2. Upon confinement to thicknesses below 100 nm, PFSI−H^+ thin-film T_T increases due to the amplified impact of substrate interaction, likely through strong hydrogen bonding between the substrate and PFSI−H^+. Addition of metal cations increases the strength of electrostatic network in the PFSI−M^+ matrix increasing physical cross-links, resulting in reduced conformational relaxation and subsequent increase in T_T, as depicted in Figure 3c. Presumably, strong ion−polymer intermolecular interactions in PFSI−M^+ appear to nullify substrate/ionomer interactions upon confinement such that T_T, α_{pre}, and α_{post} are similar to bulk PFSI−M^+ values, regardless of film thickness.

This is the first time spectroscopic ellipsometry was employed to evaluate thermal transitions in PFSI. Findings in this study confirm the strong influence of substrate and free surface upon confinement witnessed in neutralized polymer thin-films.[3,8,53,59] Increasing T_T with confinement and presence of large univalent counterions point to increased ionomer chain stiffness that could result in reduced gas permeability (see illustrations in Figures 2 and 3). In agreement with our findings, a study focusing on Cs^+ and Pt^{2+} ion-exchanged Nafion by Mohamed et al. showed greater free-volume thermal expansion in the H^+ form.[60] They also revealed chain stiffening-induced reduction in gas permeation with counterion exchange despite the higher free-volume measured. Confinement and counterion induced chain stiffening has been observed with a rise in modulus relative to bulk PFSI.[22,42,61,62] Although the polymer thickness at which the confinement effect commences does not always directly correlate with T_T deviations from the bulk value, the trend is in accord with the trends in moduli of various thin-film polymers.[6,63] Similarly, confined (<100 nm) and cation-exchanged PFSI have impeded chain mobility and increased stiffness induced by substrate interactions and physical ionic cross-links, as evidenced by their higher T_T. This can ultimately result in reduced gas permeability. Figure 4 shows this relationship between ionomer thin-film chain mobility with gas permeability utilizing data obtained from electrode diagnostics[13] and microelectrode investigations.[14] T_T of a representative electrode ionomer thin-film thickness of 46 nm was utilized to capture ionomer chain mobility at a given operating temperature ($T_T - T$); chain mobility increases as T approaches T_T. Despite the fact that the impact of water on the ionomer chain mobility was not explored here, Figure 4 shows a strong relationship between the reduction in ionomer chain mobility and the decrease in ionomer thin-film oxygen permeability.

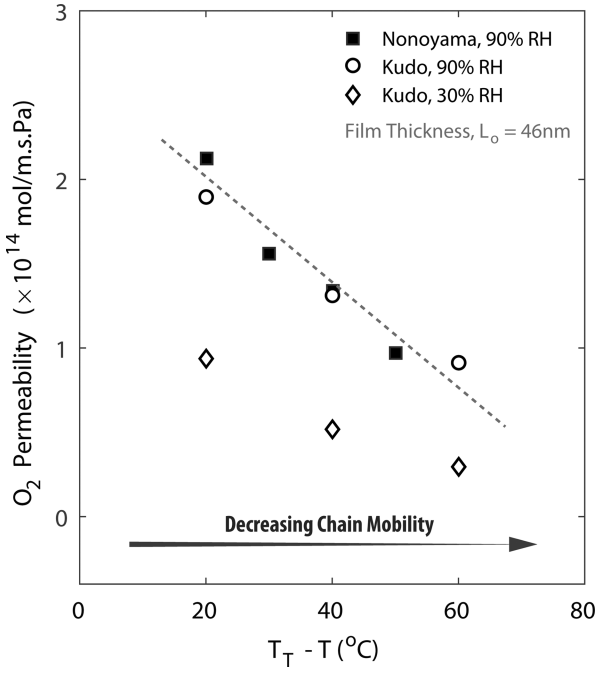

Figure 4. Nafion thin-film oxygen permeability from catalyst layer resistance[13] and microelectrode measurements[14] as a function of PFSI−H^+ thin-film (46 nm) mobility represented by $T_T - T$.

This study utilized a spectroscopic ellipsometry technique that employs a single variable (thickness variation) to characterize local changes in mobility. For expanded insights, complementary methods tracking changes in ionomer density and synergistic spectroscopic techniques that can probe molecular fluctuations especially in the presence of water are needed. Findings in this Letter signify the interplay between the surface and the electrostatic interactions controlling the thermal transitions in confined ionomer films, which could be harnessed to understand and tune ionomers' gas transport properties and functionality in porous electrodes of electrochemical energy conversion devices.

AUTHOR INFORMATION

Corresponding Authors

*E-mail: akusoglu@lbl.gov.
*E-mail: mtesfaye@berkeley.edu.

ORCID

Douglas I. Kushner: 0000-0002-3020-7737
Bryan D. McCloskey: 0000-0001-6599-2336
Adam Z. Weber: 0000-0002-7749-1624

Ahmet Kusoglu: 0000-0002-2761-1050

Notes

The authors declare no competing financial interest.

■ ACKNOWLEDGMENTS

We thank Andrew Haug and Michael Yandrasits of 3M for providing us with the PFSA dispersions and Michael Gerhardt for helpful insights and discussions. This work made use of facilities at the Joint Center for Artificial Photosynthesis supported through the Office of Science of the U.S. Department of Energy under Award Number DE-SC0004993. Funding support was supplied in part by the National Science Foundation (Grant No. DGE 1106400) and the Fuel Cell Performance and Durability Consortium (FC-PAD), by the Fuel Cell Technologies Office (FCTO), Office of Energy Efficiency and Renewable Energy (EERE), of the U.S. Department of Energy under Contract Number DE-AC02-05CH11231.

■ REFERENCES

(1) Brauman, J. I.; Szuromi, P. Thin Films. *Science (Washington, DC, U. S.)* **1996**, *273* (5277), 855.

(2) Frank, C. W.; Rao, V.; Despotopoulou, M. M.; Pease, R. F. W.; Hinsberg, W. D.; Miller, R. D.; Rabolt, J. F. Structure in Thin and Ultrathin Spin-Cast Polymer Films. *Science* **1996**, *273*, 912.

(3) Alcoutlabi, M.; McKenna, G. B. Effects of Confinement on Material Behaviour at the Nanometre Size Scale. *J. Phys.: Condens. Matter* **2005**, *17* (15), R461−R524.

(4) Rowe, B. W.; Freeman, B. D.; Paul, D. R. Physical Aging of Ultrathin Glassy Polymer Films Tracked by Gas Permeability. *Polymer* **2009**, *50* (23), 5565−5575.

(5) Rittigstein, P.; Priestley, R. D.; Broadbelt, L. J.; Torkelson, J. M. Model Polymer Nanocomposites Provide an Understanding of Confinement Effects in Real Nanocomposites. *Nat. Mater.* **2007**, *6* (4), 278−282.

(6) Torres, J. M.; Stafford, C. M.; Vogt, B. D. Elastic Modulus of Amorphous Polymer Thin Films: Relationship to the Glass Transition Temperature. *ACS Nano* **2009**, *3* (9), 2677−2685.

(7) Rowland, H. D.; King, W. P.; Pethica, J. B.; Cross, G. L. W. Molecular Confinement Accelerates Deformation of Entangled Polymers During Squeeze Flow. *Science* **2008**, *322*, 720−724.

(8) Russell, T. P.; Chai, Y. 50th Anniversary Perspective: Putting the Squeeze on Polymers: A Perspective on Polymer Thin Films and Interfaces. *Macromolecules* **2017**, *50* (12), 4597−4609.

(9) Napolitano, S.; Glynos, E.; Tito, N. B. Glass Transition of Polymers in Bulk, Confined Geometries, and near Interfaces. *Rep. Prog. Phys.* **2017**, *80* (3), 1−51.

(10) Askar, S.; Torkelson, J. M. Stiffness of Thin, Supported Polystyrene Films: Free-Surface, Substrate, and Confinement Effects Characterized via Self-Referencing Fluorescence. *Polymer* **2016**, *99*, 417−426.

(11) Gottesfeld, S.; Raistrick, I. D.; Srinivasan, S. Oxygen Reduction Kinetics on a Platinum RDE Coated with a Recast Nafion Film. *J. Electrochem. Soc.* **1987**, *134* (6), 1455−1462.

(12) Parthasarathy, A.; Srinivasan, S.; Appleby, A. J.; Martin, C. R. Electrode-Kinetics of Oxygen Reduction at Carbon-Supported and Unsupported Platinum Microcrystallite Nafion(R) Interfaces. *J. Electroanal. Chem.* **1992**, *339* (1−2), 101−121.

(13) Nonoyama, N.; Okazaki, S.; Weber, A. Z.; Ikogi, Y.; Yoshida, T. Analysis of Oxygen-Transport Diffusion Resistance in Proton-Exchange-Membrane Fuel Cells. *J. Electrochem. Soc.* **2011**, *158* (4), B416−B423.

(14) Kudo, K.; Jinnouchi, R.; Morimoto, Y. Humidity and Temperature Dependences of Oxygen Transport Resistance of Nafion Thin Film on Platinum Electrode. *Electrochim. Acta* **2016**, *209*, 682−690.

(15) Suzuki, T.; Kudo, K.; Morimoto, Y. Model for Investigation of Oxygen Transport Limitation in a Polymer Electrolyte Fuel Cell. *J. Power Sources* **2013**, *222*, 379−389.

(16) Ohira, A.; Kuroda, S.; Mohamed, H. F. M.; Tavernier, B. Effect of Interface on Surface Morphology and Proton Conduction of Polymer Electrolyte Thin Films. *Phys. Chem. Chem. Phys.* **2013**, *15*, 11494−11500.

(17) Kusoglu, A.; Kushner, D.; Paul, D. K.; Karan, K.; Hickner, M. a.; Weber, A. Z. Impact of Substrate and Processing on Confi Nement of Nafi on Thin Films. *Adv. Funct. Mater.* **2014**, *24* (30), 4763−4774.

(18) Nagao, Y. Proton-Conductivity Enhancement in Polymer Thin Films. *Langmuir* **2017**, *33* (44), 12547−12558.

(19) DeCaluwe, S. C.; Kienzle, P. A.; Bhargava, P.; Baker, A. M.; Dura, J. A. Phase Segregation of Sulfonate Groups in Nafion Interface Lamellae, Quantified via Neutron Reflectometry Fitting Techniques for Multi-Layered Structures. *Soft Matter* **2014**, *10* (31), 5763−5776.

(20) Kusoglu, A.; Dursch, T. J.; Weber, A. Z. Nanostructure/Swelling Relationships of Bulk and Thin-Film PFSA Ionomers. *Adv. Funct. Mater.* **2016**, *26* (27), 4961−4975.

(21) Frieberg, B. R.; Page, K. A.; Graybill, J. R.; Walker, M. L.; Stafford, C. M.; Stafford, G. R.; Soles, C. L. Mechanical Response of Thermally Annealed Nafion Thin Films. *ACS Appl. Mater. Interfaces* **2016**, *8* (48), 33240−33249.

(22) Page, K. A.; Kusoglu, A.; Stafford, C. M.; Kim, S.; Kline, R. J.; Weber, A. Z. Confinement-Driven Increase in Ionomer Thin-Film Modulus. *Nano Lett.* **2014**, *14* (5), 2299−2304.

(23) Paul, D. K.; Shim, H. K. K.; Giorgi, J. B.; Karan, K. Thickness Dependence of Thermally Induced Changes in Surface and Bulk Properties of Nafion ® Nanofilms. *J. Polym. Sci., Part B: Polym. Phys.* **2016**, *54* (13), 1267−1277.

(24) Tesfaye, M.; MacDonald, A. N.; Dudenas, P. J.; Kusoglu, A.; Weber, A. Z. Exploring Substrate/Ionomer Interaction under Oxidizing and Reducing Environments. *Electrochem. Commun.* **2018**, *87* (January), 86−90.

(25) DeCaluwe, S. C.; Baker, A. M.; Bhargava, P.; Fischer, J. E.; Dura, J. A. Structure-Property Relationships at Nafion Thin-Film Interfaces: Thickness Effects on Hydration and Anisotropic Ion Transport. *Nano Energy* **2018**, *46*, 91−100.

(26) Weber, A. Z.; Kusoglu, A. Unexplained Transport Resistances for Low-Loaded Fuel-Cell Catalyst Layers. *J. Mater. Chem. A* **2014**, *2* (c), 17207−17211.

(27) Yampolskii, Y.; Pinnau, I.; Freeman, B. D. Transport of Gases and Vapors in Glassy and Rubbery Polymers. *Materials Science of Membranes for Gas and Vapor Separation*; John Wiley and Sons, 2006; pp 1−48.

(28) Shimizu, R.; Park, Y.-C.; Kakinuma, K.; Iiyama, A.; Uchida, M. Effects of Both Oxygen Permeability and Ion Exchange Capacity for Cathode Ionomers on the Performance and Durability of Polymer Electrolyte Fuel Cells. *J. Electrochem. Soc.* **2018**, *165* (6), F3063−F3071.

(29) Mohamed, H. F. M.; Ito, K.; Kobayashi, Y.; Takimoto, N.; Takeoka, Y.; Ohira, A. Free Volume and Permeabilities of O2 and H2 in Nafion Membranes for Polymer Electrolyte Fuel Cells. *Polymer* **2008**, *49* (13−14), 3091−3097.

(30) Buchi, F. N.; Wakizoe, M.; Srinivasan, S. Microelectrocle Investigation of Oxygen Permeation in Perfluorinatecl Proton Exchange Membranes with Different Equivalent Weights. *J. Electrochem. Soc.* **1996**, *143* (3), 927−932.

(31) Keddie, J. L.; Jones, R. A. L.; Cory, R. A. Size-Dependent Depression of the Glass Transition Temperature in Polymer Films. *Europhys. Lett.* **1994**, *27* (1), 59−64.

(32) Frank, B.; Gast, A. P.; Russell, T. P.; Brown, H. R.; Hawker, C. Polymer Mobility in Thin Films. *Macromolecules* **1996**, *29* (20), 6531−6534.

(33) Fried, J. R.; Sadat-Akhavi, M.; Mark, J. E. Molecular Simulation of Gas Permeability: Poly(2,6-Dimethyl-1,4-Phenylene Oxide). *J. Membr. Sci.* **1998**, *149* (1), 115−126.

(34) Osborn, S. J.; Hassan, M. K.; Divoux, G. M.; Rhoades, D. W.; Mauritz, K. a.; Moore, R. B. Glass Transition Temperature of

Perfluorosulfonic Acid Ionomers. *Macromolecules* **2007**, *40* (10), 3886−3890.
(35) Matos, B. R.; Dresch, M. A.; Santiago, E. I.; Linardi, M.; de Florio, D. Z.; Fonseca, F. C. Nafion -Relaxation Dependence on Temperature and Relative Humidity Studied by Dielectric Spectroscopy. *J. Electrochem. Soc.* **2013**, *160* (1), F43−F48.
(36) Kyu, T.; Hashiyama, M.; Eisenberg, A. Dynamic Mechanical Studies of Partially Ionized and Neutralized Nafion Polymers. *Can. J. Chem.* **1983**, *61*, 680−687.
(37) Page, K. A.; Cable, K. M.; Moore, R. B. Molecular Origins of the Thermal Transitions and Dynamic Mechanical Relaxations in Perfluorosulfonate Ionomers. *Macromolecules* **2005**, *38* (15), 6472−6484.
(38) Kusoglu, A.; Weber, A. Z. New Insights into Perfluorinated Sulfonic-Acid Ionomers. *Chem. Rev.* **2017**, *117* (3), 987−1104.
(39) Mauritz, K. a.; Moore, R. B. State of Understanding of Nafion. *Chem. Rev.* **2004**, *104* (10), 4535−4585.
(40) Page, K. A.; Landis, F. A.; Phillips, A. K.; Moore, R. B. SAXS Analysis of the Thermal Relaxation of Anisotropic Morphologies in Oriented Nafion Membranes. *Macromolecules* **2006**, *39* (11), 3939−3946.
(41) Fan, Y.; Tongren, D.; Cornelius, C. J. The Role of a Metal Ion within Nafion upon Its Physical and Gas Transport Properties. *Eur. Polym. J.* **2014**, *50*, 271−278.
(42) Shi, S.; Weber, A. Z.; Kusoglu, A. Electrochimica Acta Structure-Transport Relationship of Perfluorosulfonic-Acid Membranes in Different Cationic Forms. *Electrochim. Acta* **2016**, *220*, 517−528.
(43) Pixton, M. R.; Paul, D. R.; Yampol'skii, Y. Relationships between Structure and Transport Properties for Polymers with Aromatic Backbones. In *Polymeric Gas Separation Membranes*; CRC Press: Boca Raton, FL, 1994; pp 83−154.
(44) Dalnoki-Veress, K.; Forrest, J. a.; Murray, C.; Gigault, C.; Dutcher, J. R. Molecular Weight Dependence of Reductions in the Glass Transition Temperature of Thin, Freely Standing Polymer Films. *Phys. Rev. E: Stat. Phys., Plasmas, Fluids, Relat. Interdiscip. Top.* **2001**, *63* (3), 031801−1−10.
(45) Hall, D. B.; Miller, R. D.; Torkelson, J. M. Molecular Probe Techniques for Studying Diffusion and Relaxation in Thin and Ultrathin Polymer Films. *J. Polym. Sci., Part B: Polym. Phys.* **1997**, *35*, 2795−2802.
(46) Buenviaje, C.; Dinelli, F.; Overney, R. M. Glass Transition Measurements of Ultrathin Polystyrene Films. *Techniques* **2000**, *77*, 1−18.
(47) Ho, C. Y.; Taylor, R. E. *Thermal Expansion of Solids*; ASM International, 1998; Vol. *4*.
(48) Takamatsu, T.; Eisenberg, a. Density and Expansion Coefficients of Nafion. *J. Appl. Polym. Sci.* **1979**, *24*, 2221−2235.
(49) Schaberg, M. S.; Abulu, J. E.; et al. *ECS Trans.* **2010**, *33* (1), 627−633.
(50) Hammerschmidt, J. A.; Gladfelter, W. L.; Haugstad, G. Probing Polymer Viscoelastic Relaxations with Temperature-Controlled Friction Force Microscopy. *Macromolecules* **1999**, *32* (10), 3360−3367.
(51) De Virgiliis, a.; Milchev, A.; Rostiashvili, V. G.; Vilgis, T. a. Structure and Dynamics of a Polymer Melt at an Attractive Surface. *Eur. Phys. J. E: Soft Matter Biol. Phys.* **2012**, *35* (97), 1−11.
(52) Pham, J. Q.; Green, P. F. The Glass Transition of Thin Film Polymer/Polymer Blends: Interfacial Interactions and Confinement. *J. Chem. Phys.* **2002**, *116* (13), 5801−5806.
(53) Priestley, R. D.; Ellison, C. J.; Broadbelt, L. J.; Torkelson, J. M. Structural Relaxation of Polymer Glasses at Surfaces, Interfaces, and in Between. *Science* **2005**, *309* (5733), 456−459.
(54) Burroughs, M. J.; Napolitano, S.; Cangialosi, D.; Priestley, R. D. Direct Measurement of Glass Transition Temperature in Exposed and Buried Adsorbed Polymer Nanolayers. *Macromolecules* **2016**, *49* (12), 4647−4655.
(55) Paeng, K.; Swallen, S. F.; Ediger, M. D. Direct Measurement of Molecular Motion in Freestanding Polystyrene Thin Films. *J. Am. Chem. Soc.* **2011**, *133* (22), 8444−8447.
(56) Ruhe, J.; Novotny, V.; Clarke, T.; Street, G. B. Ultrathin Perfluoropolyether Films—Influence of Anchoring and Mobility of Polymers on the Tribological Properties. *J. Tribol.* **1996**, *118* (3), 663−668.
(57) Rühe, J.; Blackman, G.; Novotny, V. J.; Clarke, T.; Street, G. B.; Kuan, S. Terminal Attachment of Perfluorinated Polymers to Solid Surfaces. *J. Appl. Polym. Sci.* **1994**, *53* (6), 825−836.
(58) Yeo, S. C.; Eisenberg, A. Physical Properties and Supermolecular Structure of Perfluorinated Ion-containing (Nafion) Polymers. *J. Appl. Polym. Sci.* **1977**, *21* (4), 875−898.
(59) Priestley, R. D.; Mundra, M. K.; Barnett, N. J.; Broadbelt, L. J.; Torkelson, J. M. Effects of Nanoscale Confinement and Interfaces on the Glass Transition Temperatures of a Series of Poly(n-Methacrylate) Films. *Aust. J. Chem.* **2007**, *60* (10), 765−771.
(60) Mohamed, H. F. M.; Kobayashi, Y.; Kuroda, C. S.; Ohira, A. Free Volume and Gas Permeation in Ion-Exchanged Forms of the Nafion Membrane. *J. Phys. Conf. Ser.* **2010**, *225*, 1−8.
(61) Albe, N. D.; Bas, C.; Reymond, L.; Dane, A.; Rossinot, E.; Flandin, L. Key Counter Ion Parameters Governing Polluted Nafion Membrane Properties. *J. Polym. Sci., Part B: Polym. Phys.* **2009**, *47* (14), 1381−1392.
(62) Page, K. A.; Shin, J. W.; Eastman, S. A.; Rowe, B. W.; Kim, S.; Kusoglu, A.; Yager, K. G.; Stafford, G. R. In Situ Method for Measuring the Mechanical Properties of Nafion Thin Films during Hydration Cycles. *ACS Appl. Mater. Interfaces* **2015**, *7* (32), 17874−17883.
(63) Tweedie, C. A.; Constantinides, G.; Lehman, K. E.; Brill, D. J.; Blackman, G. S.; Van Vliet, K. J. Enhanced Stiffness of Amorphous Polymer Surfaces under Confinement of Localized Contact Loads. *Adv. Mater.* **2007**, *19* (18), 2540−2546.